

ICSV14
Cairns • Australia
9-12 July, 2007



SOME RESULTS ON CONTROL OF SOUND RADIATION USING SHUNT PIEZOELECTRIC MATERIALS

Stanislaw J. Pietrzko, Qibo Mao

Empa – Swiss Federal Laboratories for Materials Testing and Research
Ueberlandstrasse 129, CH-8600 Dübendorf, Switzerland
stanislaw.pietrzko@empa.ch

Abstract

In this paper, several shunt piezoelectric damping techniques will be considered. Different types of shunt circuits, employed in the passive damping arrangement, will be analyzed and compared from a theoretical perspective. By using the impedance method, the piezoelectric shunt circuit can be seen as additional frequency-dependence damping of the system. By minimization of the sound power of the structure, the optimal parameters for shunt circuits can be obtained. Also, the switch law for pulse-switching circuit will be discussed based on the energy dissipation technique. Numerical simulations will be performed for each of these shunts techniques focusing on minimizing of radiated sound power from a plate. Experimental results will be presented using a RL series/parallel shunt circuit, a $RL-C$ parallel shunt circuit and pulse-switching circuit. The results show that the vibration of a structure and noise radiation can be reduced significantly by using these shunt circuits.

1. INTRODUCTION

In the early 1990's, Hagood and Flotow [1] introduced the concept of shunt piezoelectric damping. They demonstrated that it is possible to add damping to vibrating structures by using piezoelectric elements with passive shunt circuits. Piezoelectric elements were employed here to convert the mechanical energy of a vibrating structure to electrical energy which can be dissipated through the resistive components of the shunt circuit. The shunt piezoelectric damping technique does not require an external sensor. Hence, no external energy is added and the stability of the system can be guaranteed.

Following in the footsteps of Hagood and Flotow [1], many types of shunt circuits, such as RL parallel [2 – 5], $RL-C$ parallel [3, 6] and the switching shunt circuit [7 – 10], have been proposed. Typical shunt circuits are shown in Fig. 1. In general, the passive shunt circuit techniques are an effective method of modal damping. However, the main drawback of the passive shunt circuit is that shunt piezoelectric circuits are very sensitive to tuning errors and variations in the excitation frequency. To overcome this problem, Corr and Clark [7] proposed pulse-switching shunt piezoelectric circuits for structural damping. In pulse-switching, the piezoelectric element is connected to an RL shunt circuit. This allows a generated charge to be applied to the piezoelectric element; similar to direct velocity feedback control.

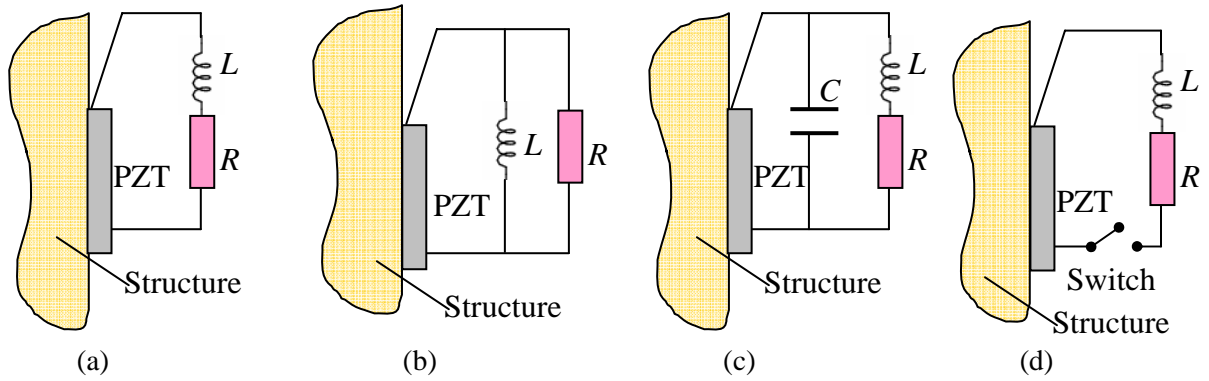


Fig. 1 Several typical piezoelectric shunt circuit. (a) RL series; (b) RL parallel; (c) $RL-C$ parallel; (d) pulse-switching.

In this study, fundamental modelling techniques for different shunt piezoelectric damping circuits such as RL series circuits, RL parallel circuits and $RL-C$ circuits are presented. Then, based on minimizing sound power of the structure, the optimal parameters for shunt circuits are discussed. The switch-law for pulse switching circuits is also considered in this study, and the detailed numerical calculations are given and discussed. Finally, with the example of a clamped plate, experimental results are given by applying RL series/parallel and pulse-switching circuits.

2. SHUNT PIEZOELECTRIC

A piezo-structure is defined as a structure consisting of embedded or bonded piezoelectric devices. The dynamic modal of the piezo-structure includes the electrical inputs and outputs as well as the modified mass stiffness effect of the structural system due to the additional piezoelectric device. A shunt circuit with a piezoelectric element can be seen as a shunt impedance Z_{sh} , as shown Fig. 2.

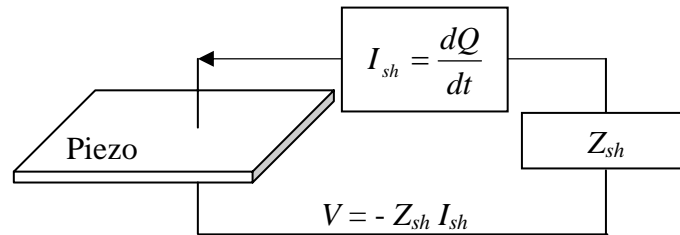


Fig. 2 Feedback current into a PZT due to shunt impedance.

Using Hamilton's principle, the mechanical and electrical equation of the system can be obtained as follows

$$[\mathbf{M}_s + \mathbf{M}_{pz}] \ddot{\boldsymbol{\eta}} + \mathbf{B} \dot{\boldsymbol{\eta}} + [\mathbf{K}_s + \mathbf{K}_{pz}] \boldsymbol{\eta} - \mathbf{coup} \cdot V = \mathbf{f} \quad (1)$$

$$Q = \mathbf{coup}^T \boldsymbol{\eta} + C_p V \quad (2)$$

\mathbf{M}_s and \mathbf{M}_{pz} are the mass matrices associated with the structure and piezoceramics, respectively. \mathbf{K}_s and \mathbf{K}_{pz} are the stiffness matrices associated with the structure and piezoceramics, respectively. \mathbf{coup} is an electromechanical coupling matrix. \mathbf{B} is the modal mechanical damping matrix. $\boldsymbol{\eta}$ is the modal coordinate vector. V is the voltage of

piezoceramics. Q is the charge on the electrical circuit. f is modal force, and C_p is the capacitance of piezoceramics.

From Fig. 2, we can define the shunt voltage as follows

$$V = -Z_{sh}I = -Z_{sh} \frac{dQ}{dt} \quad (3)$$

The charge generated by the PZT patch due to the vibration of the base structure can be determined from Eq. (2). Substituting Eq. (3) into Eq. (2),

$$V = -Z_{sh} \left(\mathbf{coup}^T \frac{d\boldsymbol{\eta}}{dt} + C_p \frac{dV}{dt} \right) = -Z_{sh} (\mathbf{coup}^T j\omega \cdot \boldsymbol{\eta} + j\omega C_p \cdot V) \quad (4)$$

Substituting Eq. (4) into Eq.(1), yields

$$\mathbf{M}\ddot{\boldsymbol{\eta}} + \left(\mathbf{B} + \mathbf{coup} \cdot \frac{Z_{sh} \cdot \mathbf{coup}^T}{j\omega C_p Z_{sh} + 1} \right) \dot{\boldsymbol{\eta}} + \mathbf{K}\boldsymbol{\eta} = \mathbf{f} \quad (5)$$

where $\mathbf{M} = \mathbf{M}_s + \mathbf{M}_{pz}$, $\mathbf{K} = \mathbf{K}_s + \mathbf{K}_{pz}$.

From Eq.(5), the shunt piezoelectric circuit can be seen as a damper modal. Frequency dependent damping $\mathbf{B}_{sh}(\omega)$ is defined

$$\mathbf{B}_{sh}(\omega) = \mathbf{coup} \cdot \frac{Z_{sh} \cdot \mathbf{coup}^T}{j\omega C_p Z_{sh} + 1} \quad (6)$$

$$Z_{sh} = \begin{cases} j\omega L + R & \text{For series circuit} \\ \frac{j\omega LR}{j\omega L + R} & \text{For parallel circuit} \end{cases} \quad (7.a)$$

$$\text{For } RL\text{-}C \text{ shunt circuit } \mathbf{B}_{sh}(\omega) = \mathbf{coup} \cdot \frac{Z_{sh} \cdot \mathbf{coup}^T}{j\omega C_T Z_{sh} + 1} \text{ with } Z_{sh} = j\omega L + R, C_T = C_p + C \quad (7.b)$$

3. OPTIMAL PARAMETERS BY MINIMIZATION OF SOUND POWER

First, for simplification, we define:

$$G(Z_{sh}) = \frac{1}{C_p} + j\omega Z_{sh}, \quad \mathbf{co} = \frac{\mathbf{coup}}{C_p} \quad (8)$$

The modal coordinate vector $\boldsymbol{\eta}$ obtained in Eq.(6) can be rewritten as:

$$\boldsymbol{\eta} = \left[\mathbf{K} - \omega^2 \mathbf{M} + i\omega \mathbf{B} + C_p \cdot \mathbf{co} \cdot \mathbf{co}^T - \frac{\mathbf{co} \cdot \mathbf{co}^T}{G(Z_{sh})} \right]^{-1} \cdot \mathbf{f} \quad (9)$$

Referring to the work of Ozer and Royston's [6], we now introduce the Sherman Morrison (SM) method for matrix inversion,

$$[A + uv]^{\text{-1}} = A^{-1} - \frac{A^{-1}uv^T A^{-1}}{1 + v^T A^{-1}u} \quad (10)$$

Using Eq.(10), Eq. (9) can be rewritten as:

$$\eta = \left[A + \frac{A \cdot co \cdot co^T \cdot A}{G(Z_{sh}) - co^T A \cdot co} \right] \cdot f = A \cdot f + \left[\frac{A \cdot co \cdot co^T \cdot A}{G(Z_{sh}) - co^T A \cdot co} \right] \cdot f \quad (11)$$

where $A = [K - \omega^2 M + i\omega B + C_p \cdot co \cdot co^T]^{-1}$.

From Eq. (11), the modal coordinate vector of the plate with a shunt piezoelectric patch can be rewritten as:

$$\eta = A \cdot f + F(Z_{sh}) \cdot [A \cdot co \cdot co^T \cdot A] \cdot f = \eta_p + F(Z_{sh}) \cdot K \quad (12)$$

where $K = [A \cdot co \cdot co^T \cdot A] \cdot f$. $F(Z_{sh}) = \frac{1}{G(Z_{sh}) - co^T A \cdot co}$, is the coefficient for optimal. η_p is the modal coordinate vector due to the primary source.

The sound power can be expressed as

$$W = \eta^H R \eta \quad (13)$$

where R is the radiation translation matrix. Substituting Eq.(12) into Eq.(13), we obtain

$$W = (\eta_p + KF)^H R (\eta_p + KF) = F^H K^H R K F + F^H (K^H R \eta_p) + (K^H R \eta_p)^H F + \eta_p^H R \eta_p \quad (14)$$

Eq.(14) is a standard Hermitian quadratic equation, using linear quadratic optimal control theory, it is easy to obtain the unique global minimum for Eq.(14), and then we can obtain the optimal inductance and resistance values for the different shunt piezoelectric circuits.

4. SWITCH LAW FOR PULSE SWITCHING CIRCUIT

In this section, the switch law for pulse switching circuits is discussed. The model of the circuit is shown in Fig. 1(d). Recall Eq.(1) and (2), if the switch is shut (meaning turned on),

$$M\ddot{\eta} + B\dot{\eta} + K\eta - \frac{coup}{C}Q + \frac{coupcoup^T}{C}\eta = f \quad (15)$$

The charge produce by the PZT actuator is:

$$L\ddot{Q} + R\dot{Q} + \frac{1}{C_p}Q = \frac{coup^T}{C_p}\eta \quad (16)$$

Assume $\mathbf{co} = \mathbf{coup}/C_p$ and substituting Eq.(16) into Eq.(15) yields

$$\mathbf{M}\ddot{\eta} + \mathbf{B}\dot{\eta} + \left[\mathbf{K} + C_p \cdot \mathbf{co} \cdot \mathbf{co}^T - \frac{\mathbf{co} \cdot \mathbf{co}^T}{\frac{1}{C_p} - \omega^2 L + i\omega R} \right] \eta = \mathbf{f} \quad (17)$$

It is assumed that the charge applied on the PZT actuator remains constant while the switch is open. The equations for the open-state can be written as:

$$\mathbf{M}\ddot{\eta} + \left[\mathbf{B} + \frac{-\mathbf{co} \cdot \mathbf{co}^T}{\frac{1}{C_p} - \omega^2 L + i\omega R} \frac{\eta_0}{\dot{\eta}} \right] \dot{\eta} + [\mathbf{K} + C_p \cdot \mathbf{co} \cdot \mathbf{co}^T] \eta = \mathbf{f} \quad (18)$$

where η_0 is the modal displacement at the time the shunt switch is opened

The fundamental issue regarding a switching circuit is to determine when to switch. From Eq.(18), maximum damping of the structure is added, if and only if

$$\eta_0 \cdot \text{sign}(\dot{\eta}) \leq 0 \quad \text{and} \quad \eta_0 = \max|\eta| \quad (\text{When switch-off}) \quad (20)$$

The natural frequency of the electric circuit is $\omega_{sh} = 1/\sqrt{LC_p}$. Assume that the inductance L is quite small and $\omega_{sh} \gg \omega_0$, from Eq.(19) and (20), it is found that η_0 reaches the first maximum at switch time

$$\Delta T_{sh} = \pi\sqrt{LC_p} = 1/2 \text{ of the period of the electric circuit} \quad (21)$$

According to Eq. (20) and (21), we can obtain the switch law for pulse switching circuit.

5. NUMERICAL CALCULATION

Assume that the piezoelectric element (20mm × 20mm) is bonded on a clamped plate with size 205mm × 205mm × 1mm. The density and Young's modulus of the plate are 1550kg/m³ and 2.75 × 10¹⁰ N/m², respectively. Assume that the damping ratio of each structural mode is 0.5%. The plate is excited by uniform incident plane waves, so only the "odd, odd" modes can be excited. The center of the PZT is located at (30mm, 30mm). The sound power of the plate is calculated to check the control performance of the different shunt circuits. Fig. 3 shows the control performances of the RL series and RL parallel circuits. It can be shown that the RL series and RL parallel circuits have the same control performance. Fig. 4 shows the control performance of the $RL-C$ parallel shunt circuit. By using the $RL-C$ parallel circuit, the

inductance value can be reduced; however, the control performance will be reduced at the same time. This situation can be viewed as a trade-off between desired component reduction and tolerable performance loss.

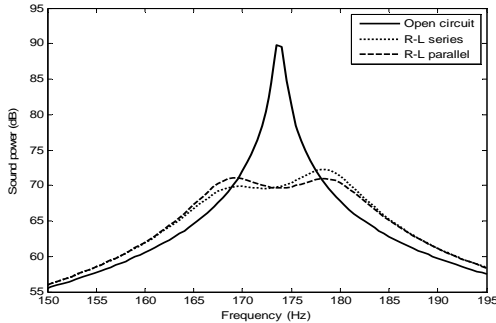


Fig. 3 The control performance of RL series and RL parallel circuit.

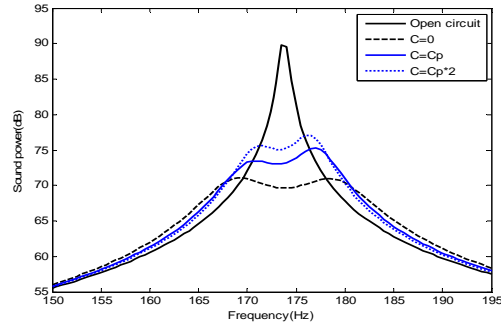


Fig. 4 The control performance of RL - C parallel circuit.

Next, we discuss the control performance of the pulse switching circuit. For a switching shunt circuit, a fundamental question considered here is when to switch. To answer this question, we show the calculated results in the time-domain. Fig. 5 compares the time response for different shunt circuits. It is found that the control performances of the RL and pulse-switching circuits are almost the same. It should be noted that the optimal inductance required is 4.17H; however, it is only 208mH for a pulse switching circuit.

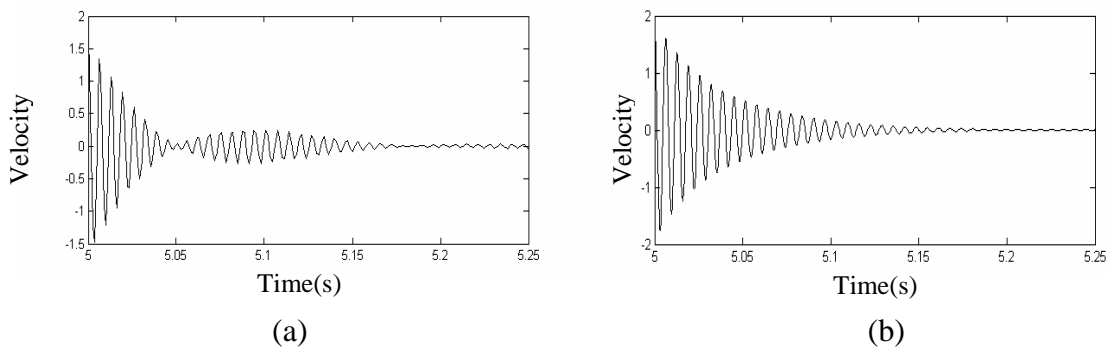


Fig. 5 Time response of the different shunt circuits (Sinusoidal burst finishing at $t=5$ s). (a) RL series circuit; (b) pulse switch circuit.

In the pulse switch circuit, the actuator is switched to an RL shunt circuit when the modal velocity is zero. As the charge of the PZT actuator reaches a peak that is opposite in sign to that which it began as, the switch is opened and the charge remains constant until the switch closes again. The applied charge is 180° out of phase with modal velocity over each switch-open time. This is directly analogous to the well-known, direct velocity feedback control system (DVFB). The only difference between a pulse-switch and DVFB is that for DVFB, the applied voltage varies over the half cycle, and for a pulse-switch, the applied charge is constant over the half cycle. Fig. 6 compares the control performances between the RL series and pulse-switching circuits. When the stiffness of a structure is changed, the performance of the pulse-switching circuit remains about 7dB. However, the performance of the RL series circuit degrades quickly; the maximum sound power reduction is achieved only when the RL shunt circuit is precisely tuned to the required frequency of concern. This means that a pulse-switching circuit is more stable than a RL series circuit with regard to stiffness variations.

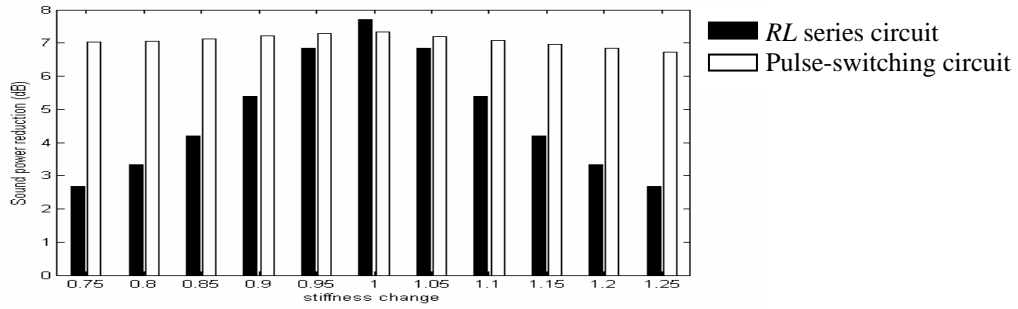


Fig. 7 Comparison of the control performance between *RL* series and pulse-switching circuits.

6. EXPERIMENT SETUP AND RESULTS

In order to demonstrate the control performance of the *RL* series, *RL* parallel, *RL-C* parallel and pulse-switching shunt techniques, an experimental test was performed on a clamped steel plate. This experiment is intended to demonstrate each of the four shunt circuits and to compare them in a real vibrating system. A 200mm × 200mm × 2mm steel plate with two piezoelectric QP25W elements (one is used as primary source and another for the shunt circuit), one piezo-fiber sensor which is used to drive switch controller, and one accelerometer bonded to its surface (center of the plate) were used to monitor the control performance for each test. The plate was clamped at all boundaries.

All frequency response functions (FRFs) were measured, from the voltage output of the accelerometer to the voltage input the primary PZT actuator. A PULSE dynamic signal analysis system was employed to create the excitation signal and perform all FRFs measurements. The goal of the experiment was to control the second structural mode (with a natural frequency 340Hz) of the plate by using a different shunt circuit. Tab.1 lists the values of the components used for each of the shunt circuits. All inductors used in the shunt circuits were passive inductors.

Tab.1 Properties of shunt circuits used in experiments

	<i>RL</i> series	<i>RL</i> parallel	<i>RL-C</i> parallel	Pulse-switching
Resistance (Ω)	55	31K	28	10
Inductance (H)	0.71	0.72	0.445	0.071
Capacitance (μF)	None	None	0.2	None

In the first test, the control performance of *RL* series, *RL* parallel and *RL-C* parallel circuits was tested. The results are shown in Fig. 7. Fig. 7 indicates that the shunt piezoelectric element can significantly reduce the resonant peak vibrations. Furthermore, the results also show that the control performances of *RL* series and *RL* parallel circuit are basically the same. With *RL-C* parallel circuits, the additional capacitance can reduce the value of inductance (See Tab. 1); however, the control performance has also been reduced due to the additional capacitance as shown in Fig.16.

Fig. 8 shows the experimental result employing a pulse-switching circuit. It can be shown that a pulse-switching circuit can achieve the same control performance as the *RL* series circuit. By using a pulse-switching circuit, the value of the inductance can be reduced to 0.071H (10% of *RL* series circuit). The advantages of the switching techniques are a small required shunt inductance, a lower sensitivity to environmental changes and easier tuning.

Very low external power for the switch controller is required so it may be possible to extract this energy directly from the vibration of the structure itself.

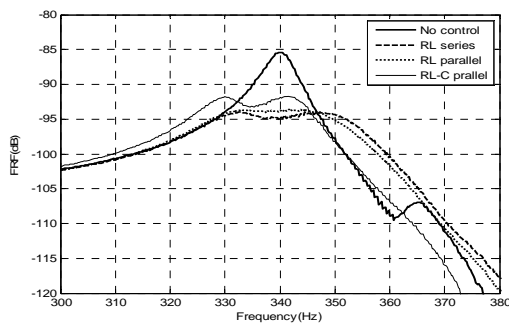


Fig. 7 Experimental comparison of RL series and parallel shunt circuits.

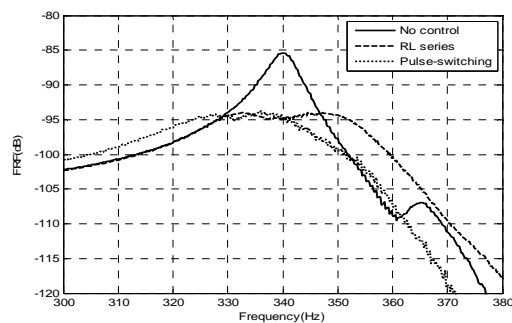


Fig. 8 Experimental comparison of RL series and pulse-switching circuits.

7. CONCLUSIONS

In this study, several different shunt piezoelectric damping techniques, i.e. RL series, RL parallel, $RL-C$ parallel and pulse-switching shunt circuit, have been analyzed and compared. By using the impedance method, the piezoelectric shunt circuit can be seen as additional frequency-dependence damping of the system. By minimization of the sound power of the structure, the optimal parameters for shunt circuits have been obtained. Also, the switch law for pulse-switching circuits have been discussed. Numerical simulations were performed for each of these shunts techniques. It was found that the RL series and RL parallel circuit have basically the same control performance. Experimental results have been presented using a RL series shunt circuit, a $RL-C$ parallel shunt circuit and pulse-switching circuit. These results have shown that the vibration of a structure can be reduced significantly by using these shunt circuits. The theoretical and experimental techniques presented in this study provide a valuable tool for effective shunt piezoelectric damping.

REFERENCES

- [1] N. W. Hagood and A. V. Flotow. Damping of structural vibration with piezoelectric materials and passive electrical networks. *J. Sound Vib.* **146**, 243 – 268 (1991).
- [2] S. Y. Wu. Piezoelectric shunts with parallel R-L circuit for smart structural damping and vibration control. *Proc. SPIE Smart Struct Conf.: Passive Damping Isolation. Mater.* 259 – 269 (1996).
- [3] G. Caruso. A critical analysis of electric shunt circuits employed in piezoelectric passive vibration damping. *Smart Mater. Struct.* **10**, 1059 – 1068 (2001).
- [4] C. H. Park. Dynamics modelling of beams with shunted piezoelectric elements. *J. Sound Vib.* **268**, 115–129 (2003).
- [5] A. Agneni, F. Mastroddi, G.M. Polli. Shunted piezoelectric patches in elastic and aeroelastic vibrations. *Computers and Structures.* **81**, 91–105 (2003).
- [6] M. B. Ozer and T. J. Royston. Passively minimizing structural sound radiation using shunted piezoelectric materials. *J. Acoust. Soc. Am.* **114**, 1934 – 1946 (2003).
- [7] W. W. Clark. Vibration control with state-switching piezoelectric materials. *J. Intell. Mater. Syst. Struct.* **11**, 263–271 (2000).
- [8] R. C. Lawrence and W. W. Clark. Comparison of low-frequency piezoelectric switching shunt techniques for structures damping. *Smart Mater. Struct.* **11**, 370 – 376 (2002).
- [9] R. C. Lawrence and W. W. Clark. A novel semi-active multi-modal vibration control law for a piezoceramic actuator. *Trans. ASME. J. Vib. Acoust.* **125**, 214 – 222 (2003)
- [10] R. C. Lawrence and W. W. Clark. Energy dissipation analysis of piezoceramic semi-active vibration control. *J. Intell. Mater. Syst. Struct.* **12**, 729 – 736 (2001).